

Quantum wave bandstop filters

Y. Wang and S. Y. Chou

Department of Electrical Engineering, University of Minnesota, Minneapolis, Minnesota 55455

(Received 3 May 1994; accepted for publication 12 August 1994)

We propose and demonstrate, based on the concept of a microwave bandstop filter, two quantum wave bandstop filter structures. Both structures employ nanoscale gates in a heterojunction transistor to induce a quantum cavity connected by two one-dimensional wires. As the electron wavelength is changed by the gate voltage, we observed that, at certain gate voltages, the transmission of electron waves through the cavity is partially blocked and the drain current drops as large as 50%. This phenomenon is explained in terms of the destructive quantum interference between different electron wave modes in the cavity. © 1994 American Institute of Physics.

Because of the similarity between electron waves in a quantum waveguide and electromagnetic waves in a microwave waveguide, many microwave device concepts can be instructive in engineering new high functionality quantum devices.¹ Previously, several structures based on such analogy have been proposed and discussed.²⁻⁸ Examples are a stub-tuning device,²⁻⁵ a double-bend quantum waveguide,⁶ and a cavity coupled to two quantum waveguides.⁶⁻⁸ However, most of these studies were limited to the computer simulations and theoretical analysis. Experimentally, only in stub-tuning devices, weak conductance modulations as a function of gate voltage were observed and attributed to the quantum interference effect.^{4,5} Here we propose and demonstrate, based on the concept of a microwave waveguide cavity bandstop filter, two quantum wave bandstop filter structures consisting of field-induced nanoscale cavities and one-dimensional (1D) wires. As the electron wavelength is changed by the gate voltage, we observed that, at certain gate voltages, the transmission of electron waves is partially blocked and the drain current drops drastically. This phenomenon is explained in terms of the destructive interference between different electron wave modes in the cavity.

The quantum wave filters employ two different types of nanoscale gate structures on top of a heterostructure to induce, using field effects, a quantum cavity connected by two 1D wires. The first type has a dot gate inside the gap of a split gate [Fig. 1(a)]. The dot gate has an 80-nm-diam metal dot in the middle of a 30-nm-wide metal wire. When positively biased, the dot gate induces, at the heterostructure interface underneath the gate, a nanoscale electron cavity connected by two 1D wires. The negatively biased split gate controls the electron population in the cavity and wire, and also improves the electron confinement.⁹ Since the cavity is primarily defined by the positive bias on the dot gate, it is called an enhancement mode cavity.

The second type of gate structure has a straight wire gate between a pair of U-shape split gates [Fig. 1(b)]. The negatively biased U-shape split gate depletes the electron underneath it and thus defines the cavity. The lithographic dimension of the cavity is $0.3 \mu\text{m} \times 0.5 \mu\text{m}$, the actual dimension of confinement at the heterostructure interface can be much smaller due to finite depletion width. The wire gate is positively biased to separately control the electron population in the cavity.¹⁰ In this case, the cavity is primarily defined by

the negative bias on the split gate, it is called a depletion mode cavity.

In both structures, the quantum cavity is coupled to the two-dimensional electron gas (2DEG) reservoirs on both sides through 1D wires (quantum waveguides). If the Fermi level is below the threshold of the first subband in the 1D waveguides, the 1D waveguides become barriers, and the electron transport through the structure is in tunneling regime. If the Fermi level is above the threshold of the first subband in the 1D waveguides, the electron wave can propagate through the waveguides, and the transport is in propagation regime. In this experiment, we focus on the propagation regime and study the case where only a single incident mode exists in the 1D waveguide.

The gate structures are fabricated on top of a δ -doped AlGaAs/GaAs heterostructure using electron-beam lithography followed by a lift-off of Ti/Au. The heterostructure consists of a $0.5 \mu\text{m}$ GaAs buffer layer on a semi-insulating GaAs substrate, a 20 nm undoped $\text{Al}_{0.3}\text{Ga}_{0.7}\text{As}$ spacer layer, a δ -doped layer with a Si concentration of $7 \times 10^{12} \text{ cm}^{-2}$, a 15 nm undoped $\text{Al}_{0.3}\text{Ga}_{0.7}\text{As}$ layer, and a 5 nm n -GaAs cap layer with a Si concentration of $3 \times 10^{18} \text{ cm}^{-3}$. The distance between the gate metal and the 2DEG is 40 nm. At 4.2 K in the dark, the 2DEG has a mean free path of $2 \mu\text{m}$.

The characteristic of both devices are measured at $T=0.5 \text{ K}$ in a He^3 sorption pumped refrigerator. For the enhancement mode cavity device, the split-gate voltage is fixed

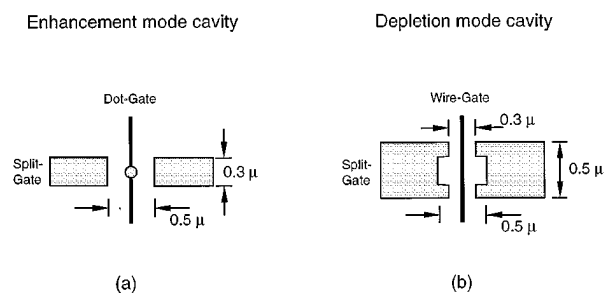


FIG. 1. Schematic diagram of the gate structures used to create a cavity coupled to two 1D waveguides. (a) An enhancement mode cavity: cavity induced by the positive bias on the dot gate. (b) A depletion mode cavity: cavity created by negative bias on the U-shape split gate.

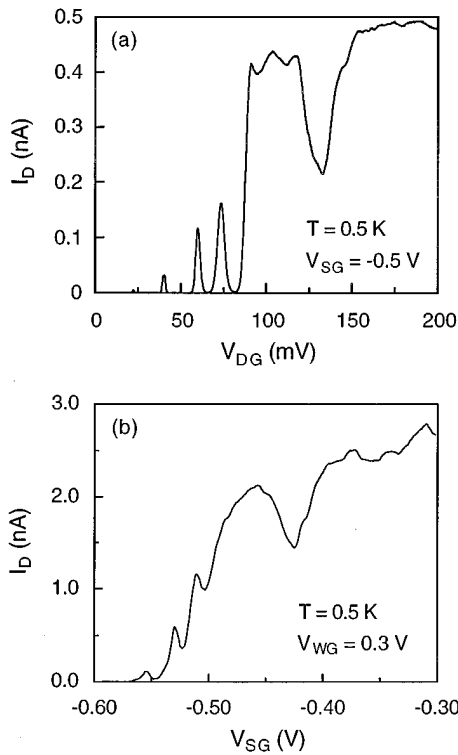


FIG. 2. The drain current measured at 0.5 K. (a) For an enhancement mode cavity, (b) for a depletion mode cavity. Each shows a current notch in the current plateau.

at -0.5 V, and the drain current is measured as the dot-gate voltage is scanned positively to change the electron wavelength. For the depletion mode cavity device, the wire gate is fixed at 0.3 V, and the drain current is measured as the split-gate voltage is scanned negatively to change the electron wavelength. The results are shown in Figs. 2(a) and 2(b). Two common features can be noted from the measurements. First, there are oscillation peaks near the onset of the current. These peaks arise from the resonant tunneling through the energy levels inside the cavity and have been discussed before.⁹ Second, in the propagation regime of both types of devices, the oscillations diminish and the current stays relatively flat except there is a deep current notch in the middle of the current plateau. Notice that the current is directly proportional to the electron transmissivity by Landaur's formula,¹¹ and the gate voltage controls the electron Fermi level hence the electron wavelength, therefore the observation of current notch at a certain range of gate voltages implies that the electron wave transmission is partially blocked for a range of electron wavelengths. In other words, the device structures have a stopband for electron waves. From Fig. 2(a) we see that, in the enhancement mode cavity, the current drops as much as 50%.

The effect of temperature on the current notch in the enhancement mode cavity is shown in Fig. 3. The measured curves are vertically displaced for clarity. As the temperature increases, the curve becomes smoother, the current notch becomes less pronounced, and finally disappears at 4.4 K.

We now show that the observed current notch can be

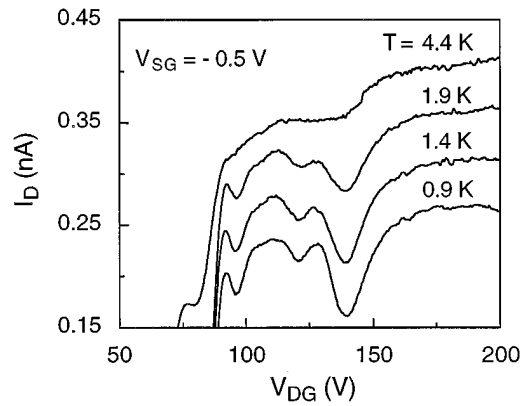


FIG. 3. Temperature effect on the current notch. As temperature increases, the current notch becomes less pronounced and disappears at 4.4 K. The curves are displaced for clarity.

explained in terms of the destructive quantum interference between different modes in the cavity. For simplicity, consider a rectangular cavity coupled to two 1D waveguides as depicted in Fig. 4(a). Inside the two 1D waveguides, there is only one transverse mode (channel) occupied; however, in the cavity, due to the wider lateral dimension, there are N channels ($N \geq 1$) below the incident electron energy. Assuming the contribution of the evanescent waves is negligible, the cavity can be replaced by N 1D channels. Then we have the following picture of the electron transport: an electron wave incident from the source into a 1D channel, branches to

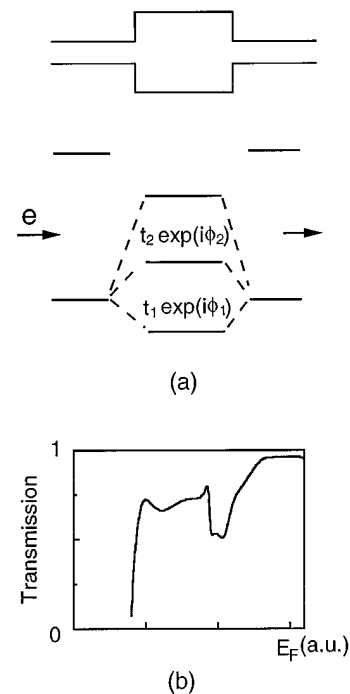


FIG. 4. (a) Schematic diagram of a rectangular cavity coupled to two 1D waveguides. In the waveguides, only one transverse mode is occupied. However, in the cavity, several transverse modes are available. (b) Calculated electron transmission through the cavity based on the simple picture of N -channel interference.

N channels, and recombine into one 1D channel as output. Thus the total electron transmission is simply a coherent sum of the transmission through each of the N channels. Notice that although all N channels have the same length, the propagation constant in each channel is different and changes as the gate voltage is scanned, therefore a complicated interference pattern is expected. It can be shown theoretically that, at zero temperature, the interference will always lead to zero transmission for certain electron energies.^{6,7} Experimentally, however, because of the finite temperature and drain bias, the transmission will never completely drop to zero. In Fig. 4(b), we show the computer simulation results based on a simple model using the dimensions close to the enhancement mode cavity shown in Fig. 1(a). The zero transmission does not occur because we have neglected the interchannel scattering in our simple model. As shown, the profile of the simulation is in reasonable agreement with the experimental curve. The details of the calculation and analysis will be published elsewhere.¹²

In summary, we have proposed and demonstrated two quantum wave bandstop filters formed by field-induced nanoscale cavities coupled to 1D wires. Both show energy filtering effects in the propagation regime at certain electron wavelengths. The phenomenon can be explained in terms of the destructive quantum interference between different electron wave modes in the cavity. This experiment demonstrates

that a quantum cavity can behave as a filter for quantum waves similarly to a microwave cavity for electromagnetic waves.

The authors would like to thank W. Y. Deng for the compute simulation and useful discussions. This work is partially supported by ONR, ARPA, and ARO

- ¹ See, for example, *Nanostructure Physics and Fabrication*, edited by M. A. Reed and W. P. Kirk (Academic, San Diego, 1990).
- ² F. Sols, M. Macucci, U. Ravaioli, and K. Hess, *Appl. Phys. Lett.* **54**, 350 (1989).
- ³ S. Datta, *Superlatt. Microstruct.* **6**, 83 (1989).
- ⁴ D. C. Miller, R. K. Lake, S. Datta, M. S. Melloch, and R. Reifenger, in Ref. 1, p. 165.
- ⁵ K. Aihara, M. Yamamoto, and T. Mizutani, *IEEE IEDM Tech. Dig.* **1992**, 491.
- ⁶ A. Weisshaar, J. Lary, S. M. Goodnick, and V. K. Tripathi, *Appl. Phys. Lett.* **55**, 2114 (1989); see also, A. Weisshaar, J. Lary, S. M. Goodnick, and V. K. Tripathi, *J. Appl. Phys.* **70**, 355 (1991).
- ⁷ C. S. Lent and S. Sivaprakasam, in *Nanostructures and Microstructure Correlation with Physical Properties of Semiconductors*, edited by H. G. Craighead and J. M. Gibson (SPIE, San Diego, CA, 1990), p. 31.
- ⁸ F. M. Peeters, in *Science and Engineering of One and Zero-Dimensional Semiconductors*, edited by S. P. Beaumont and C. M. S. Torres (Plenum, New York, 1990), p. 107.
- ⁹ Y. Wang and S. Y. Chou, *Appl. Phys. Lett.* **63**, 2257 (1993).
- ¹⁰ S. Y. Chou and Y. Wang, *Appl. Phys. Lett.* **63**, 788 (1993).
- ¹¹ R. Landauer, *IBM J. Res. Dev.* **1**, 223 (1957); see also M. Büttiker, Y. Imry, R. Landauer, and S. Pinhas, *Phys. Rev. B* **31**, 6207 (1985).
- ¹² Y. Wang, W. Y. Deng, and S. Y. Chou (unpublished).